

Analysis for EBIS Electron Collector

May 11, 2005
Revision A

Table of Contents

Part I. Hydraulic and Heat Transfer Calculations for EC	4
EC Specifications:.....	4
Hydraulic and Heat Transfer Calculations:	6
Part II. Transient Thermal FE Model of EC	10
The FE Model:	10
Transient Thermal Analysis Results:	13
Verification of Transient Thermal Response:	15
Part III. FE Model Structural Analysis	17
Mean Stresses and Stress Ranges at Start of Pulsing:	17
Mean Stresses and Stress Ranges at Steady Cycling:.....	18
Summary:	20
Part IV. Analysis of Fatigue Strength of Copper Alloys for EC	21
Considerations in Evaluating Fatigue Life:.....	21
Procedure for evaluating fatigue:	21
Conclusions:	22
Fatigue Calculation for Beryllium Copper	24
Part V. Convective Heat Transfer In the EC.....	27
Definition of Critical Heat Flux:.....	27
CHF Factors in the EC:	28
Operating Parameters of the EC:.....	28
Summary of the Heat Transfer Calculations:.....	30
Critical Heat Flux (CHF):	30
Other CHF Research:.....	31
Calculations of Convective Heat Transfer in EC:.....	32
VI. EC Materials of Construction:	42
Conclusion	44

Table of Figures

Figure 1: Electron Collector	4
Figure 2: FE Model of 6-Degree EC Segment (Half Section).....	10
Figure 3: Power Density Distribution on EC, 15kV, 20.4A	11
Figure 4: Heat Flux Distribution, FE Model	12
Figure 5: Temperature Equilibrium Plot at Node 7910	13
Figure 6: Temperature Cycling - Start of Pulsing	13
Figure 7: Temperature Distribution	14
Figure 8: Time-Temperature (Node 7910)	14
Figure 9: Heat Flux, X-dir (X-dir is toward center of channel).....	15
Figure 10: Heat Flux at EC Inside Diameter (Node 7910) and at Channel (Red – Node 10157)	15
Figure 11: Maximum Stress on EC Inside Diameter.....	17
Figure 12: Maximum Stress on EC Outside Diameter	18
Figure 13: Von Mises Stress-End of 30 mS Pulse (24.1 ksi max, dropping to 23.6 ksi)	19
Figure 14: Tangent or Hoop Stress-End of Pulse (27.4 ksi I.D. compression, dropping to 27.3 ksi)	19
Figure 15: Axial Stress-End of Pulse (9.66 ksi I.D. compression, increasing to 15.2 ksi).....	19
Figure 16: Modified Goodman Diagram for BeCu, C17510.....	26
Figure 17: EC Water/Wall Temperature Profile.....	36

Part I. Hydraulic and Heat Transfer Calculations for EC

EC Specifications:

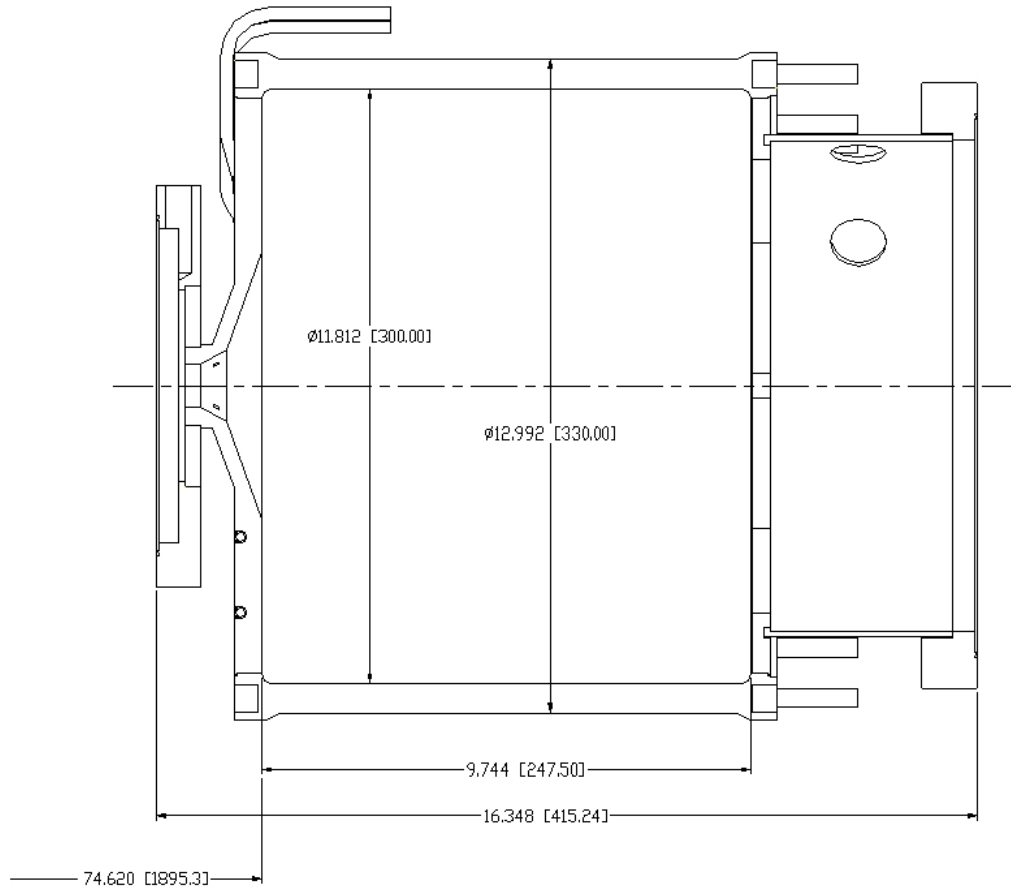


Figure 1: Electron Collector

Inside Diameter, mm	300
Outside Diameter, mm	330
Length of EC, mm	247
Cooling Channel Diameter, mm	9
Number of Cooling Flow Loops	10
Number of Flow Passes per Loop	6
Total Number of Flow Passes	60
Flow Rate per Loop, gpm (lpm)	4 (15.1)
Pulse Heat Load, kW, Max.	300 ^a

A summary of the calculations of pressure drop and heat transfer in the EC shown below are as follows:

Pressure Drop for Each Flow Loop, psi	34 ^b
Cooling Water Temperature Rise for DC beam	28 C
Length of EC Exposed to Beam (approx), mm	170
Aver Temperature Difference, Tube to Water, DC beam	95 C
Aver Heat Flux on EC Inside Diameter, watt/cm ²	187 ^c
Aver Heat Flux on Cooling Channel, watt/cm ²	104
Ratio of Channel Heated Area to EC Inside Area	1.8

Notes:

- a. The EC design heat load during the pulse is 300 kW. The average heat load for pulsed beam will be only 45kW (15%) for a 30 mS pulse at 5 hz.
- b. Pressure drop is for single-phase flow without subcooled boiling. Several references indicate that the pressure drop becomes less when subcooled boiling starts, then greater as boiling increases.
- c. The heat flux on the EC inside diameter corresponds to 300kW, uniformly distributed.

Hydraulic and Heat Transfer Calculations:

Pressure Loss through Electron Collector- (Crane Technical Paper No. 410)

Flow diameter	$d_C := 9 \cdot \text{mm}$
Flow Area	$A_C := .785 \cdot d_C^2$ $A_C = 6.359 \times 10^{-5} \text{ m}^2$
Volumetric Flow Rate -	$Q := 4 \cdot \frac{\text{gal}}{\text{min}} \quad Q = 15.142 \frac{\text{liter}}{\text{min}}$
Flow Velocity, v	$v := \frac{Q}{A_C}$ $v = 3.969 \text{ msec}^{-1}$
Kinematic Visc @ 60 degF (16 degC)	$v \equiv 1.169 \cdot 10^{-6} \cdot \frac{\text{m}^2}{\text{sec}}$
Absolute Visc @ 60 degF (16 degC)	$\mu \equiv .00112 \cdot \frac{\text{kg}}{\text{m} \cdot \text{sec}}$
Density @ 60 degF (16 degC)	$\rho_w \equiv 999.2 \cdot \frac{\text{kg}}{\text{m}^3}$
Reynolds Number	$N_{re} := \frac{d_C \cdot v}{v}$ $N_{re} = 3.056 \times 10^4$

(This Reynolds No. is in the transition zone between laminar and turbulent flow.)

friction factor (Moody Diagram)	$f := .033$
friction factor (turbulent)	$f_t := .030$

Resistance Coefficients: (k_t)

Tube Length -each loop	$L := 1722 \cdot \text{mm}$
Tube Factor, k_1	$k_1 := \left(f \cdot \frac{L}{d_c} \right)$
	$k_1 = 6.3$
Entrance, k_2	$k_2 := .5$
Exit, k_3	$k_3 := 1.0$
Elbows (12), k_4	$k_4 := 60 \cdot f_t$
	$k_t := k_1 + k_2 + k_3 + 12 \cdot k_4$
	$k_t = 29.4$

Pressure Loss:

$$h_L := k_t \cdot \left(\frac{v^2}{2} \right) \cdot \rho_w$$

$$h_L = 2.315 \times 10^5 \text{ Pa}$$

$$h_L = 33.573 \text{ psi}$$

Water Temperature Rise ($T_{out} - T_{in}$) at Peak Heat Load:

(This would be the water temperature rise at a DC (non-pulsed) condition, where $Q = mc(T_{out} - T_{in})$. The actual temperature rise will be the Δt below times the duty factor, where DF = pulse duration times pulse frequency.)

q_T = peak heat dissipated by EC	$q_T := 300 \cdot \text{kW}$
n = number of cooling loops	$n := 10$
Q = flow rate thru each loop	$Q = 15.142 \frac{\text{liter}}{\text{min}}$
c_w = specific heat of water	$c_w := 4.183 \cdot \frac{\text{joule}}{\text{gm} \cdot \text{degC}}$
q_1 = heat removed thru each loop	$q_1 := \frac{q_T}{n}$
	$q_1 = 3 \times 10^4 \text{ watt}$
m_1 = mass flow thru each loop	$m_1 := \rho_w \cdot Q$
	$m_1 = 0.252 \text{ kgsec}^{-1}$
Δt = temperature rise at DC condition	$\Delta_{t1} := \frac{q_1}{m_1 \cdot c_w}$
	$\Delta_{t1} = 28.4 \text{ degC}$

Calculation of Average Temperature Difference across Channel Wall/Water Boundary during Steady State Heat Flux for Turbulent Flow:

L_{hc} = approx heated length of collector I.D.

$$L_{hc} := 170 \cdot \text{mm}$$

p = number of passes per cooling loop

$$p := 6$$

k_w = conductivity of water @ 60 degF (16 degC)

$$k_w := .595 \cdot \frac{\text{watt}}{\text{m} \cdot \text{degC}}$$

A_{tw} = tube/water heat transfer area equals tube circum X heated length

$$A_{tw} := (\pi \cdot d_c) \cdot L_{hc} \cdot p$$

$$A_{tw} = 0.029 \text{m}^2$$

N_{pr} = Prandtl No. of water @ 60 degF (16 degC)

$$N_{pr} := 7.88$$

N_{nu} = Nusselt No.

(use Dittus-Boelter Eqn. for turbulent flow based on bulk fluid temperature from 'Heat Transfer', Chapman)

$$N_{nut} := .023 \cdot N_{re}^{.8} \cdot N_{pr}^{.3}$$

$$N_{nut} = 165.5$$

$h = N_{nu} \cdot k_w / d_c$, where h = heat transfer coefficient

$$h_t := \frac{N_{nut} \cdot k_w}{d_c}$$

$$h_t = 1.094 \times 10^4 \frac{\text{watt}}{\text{m}^2 \cdot \text{degC}}$$

Δ_{tw} = temperature difference between EC channel wall and bulk water.

$$\Delta_{tw} := \frac{q_1}{h_t \cdot A_{tw}}$$

$$\Delta_{tw} = 95.1 \text{degC}$$

Average Heat Flux (q_a) on Inside Collector Surface during Pulse, q_a

R_{col} = inside radius of collector

$$R_{col} := 150 \cdot \text{mm}$$

A_{cyl} = Inside Area of Cylindrical Collector

$$A_{cyl} := 2 \cdot \pi \cdot R_{col} \cdot L_{hc}$$

$$A_{cyl} = 0.16 \text{m}^2$$

q_{av} = average heat flux on EC I.D.:

$$q_{av} := \frac{q_T}{A_{cyl}}$$

$$q_{av} = 1.872 \frac{\text{watt}}{\text{mm}^2}$$

Ratio of Flow Area to Inner Collector Surface Area

$$R_{area} := \frac{n \cdot A_{tw}}{A_{cyl}}$$

$$R_{area} = 1.8$$

Average Heat Flux on Water Channel Area during Pulse, q_{af}

$$q_{af} := \frac{q_{av}}{R_{area}}$$

$$q_{af} = 1.04 \frac{\text{watt}}{\text{mm}^2}$$

Part II. Transient Thermal FE Model of EC

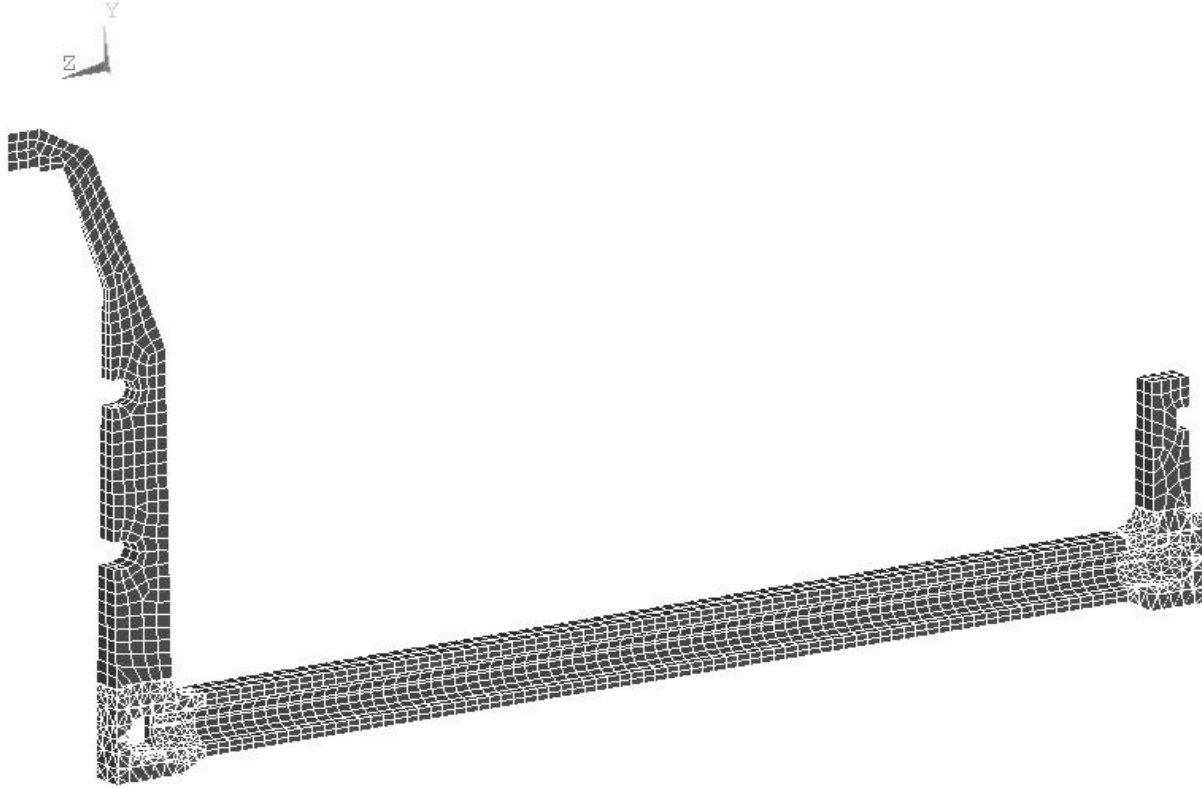


Figure 2: FE Model of 6-Degree EC Segment (Half Section)

The FE Model:

1. The model is a 6-degree segment of the cylindrical EC with symmetry boundary conditions applied. The segment is centered on one of the 60 cooling channels.
2. The material of construction is beryllium copper, C17510. The properties are as follows:

Density, kg/m ³	8,830
Specific Heat, J/kg-C	419
Modulus, E, Pa	1.38e11
Poisson Ratio	.35
Coef of Exp, ppm/C	17.7
Conductivity, W/m-C	242
Yield Strength, ksi	80-100*
Ultimate Strength, ksi	100-130*
Fatigue Strength, ksi (10 ⁸ cycles)	38-44*

*The above strengths represent the 'AT' temper, solution annealed, precipitation age hardened.

3. The inside diameter of the EC collector and the front disk face are heated by a 30mS, 5 hz pulsed electron beam. The heat flux power distribution on the inside cylindrical surface as a function of Z is shown in figure 3 below⁸. The heat flux extends from Z=1945 to 2116mm. The front inside face of the EC is at Z = 1895.3mm. The heat flux on the front disk face during the pulse is 5 kW, corresponding to 9.7 watts/cm².

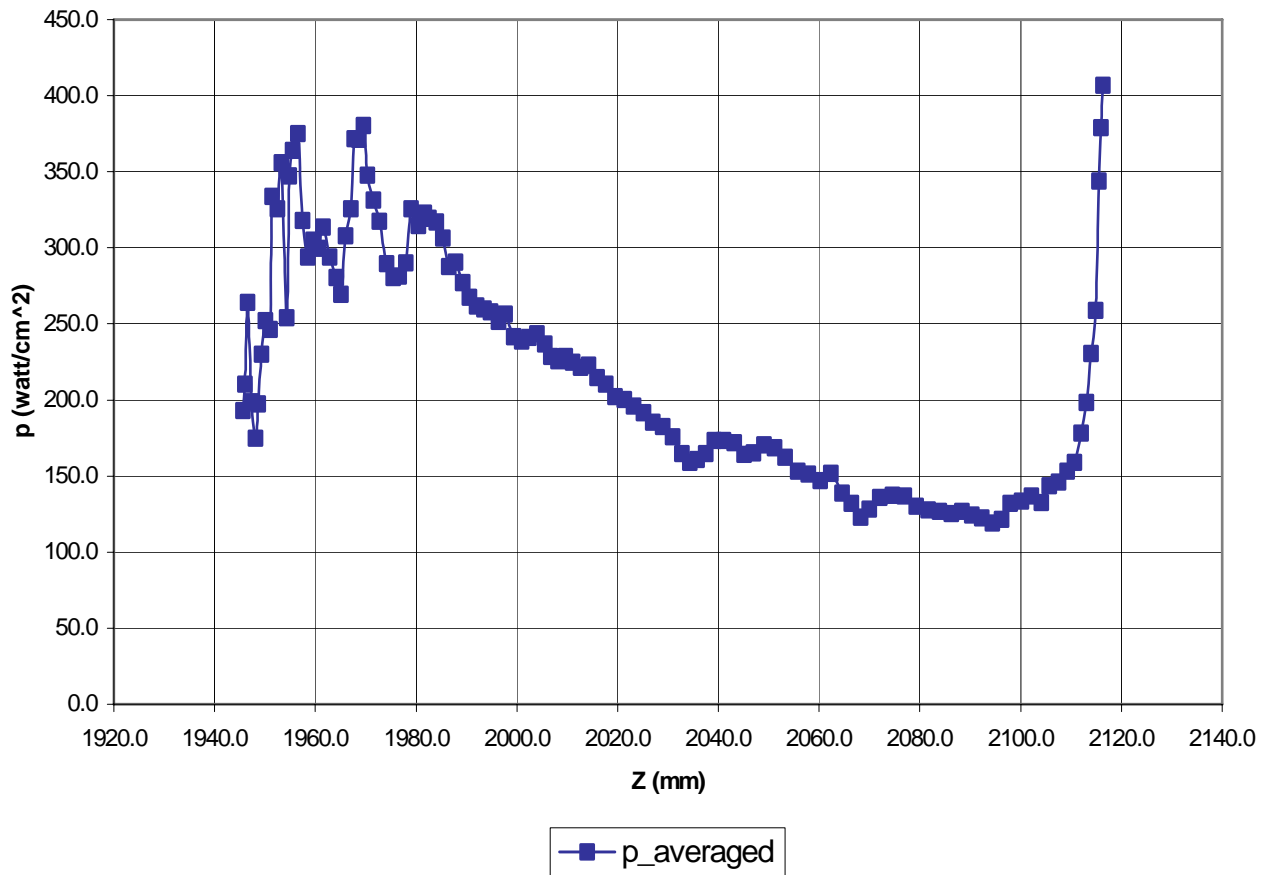


Figure 3: Power Density Distribution on EC, 15kV, 20.4A

This distribution is shown applied to the FE Model in figure 4.

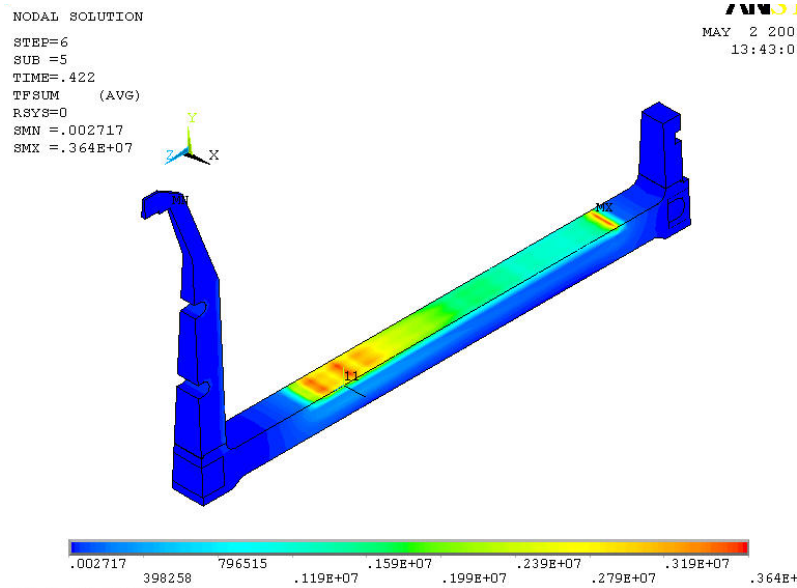


Figure 4: Heat Flux Distribution, FE Model

4. Convective cooling (calculated in part I) is applied on the inside of the water channel and at the two front disk cooling channels as an overall heat transfer coefficient equal to $1.1e4$ watt/ $m^2 \cdot C$ at a bulk water temperature of 20C.
5. The thermal transient analysis yields the following results:
Time to reach the maximum temperature distribution, the fluctuating temperature response from the pulsed beam during the first 5 cycles, and the temperature response after a long time (LT).
6. In the last case the load conditions that were applied to determine the temperature response after LT pulsing are as follows:
 - a. Load Step 1: Steady state heat flux in watts/ m^2 at the averaged pulse intensity is applied to establish an initial average temperature distribution.
 - b. Load Step 2: Apply the full pulse heat flux shown in the figure for 30 mS.
 - c. Load Step 3: Remove the heat flux for the remainder of the cycle, 170 mS.
 - d. Load Steps 4–7: Repeat LS 2 and LS 3 for two more cycles.

Transient Thermal Analysis Results:

1. The time for the EC to reach thermal equilibrium is approximately 10 seconds. Figure 5 shows the average temperature versus time at highest temperature node.

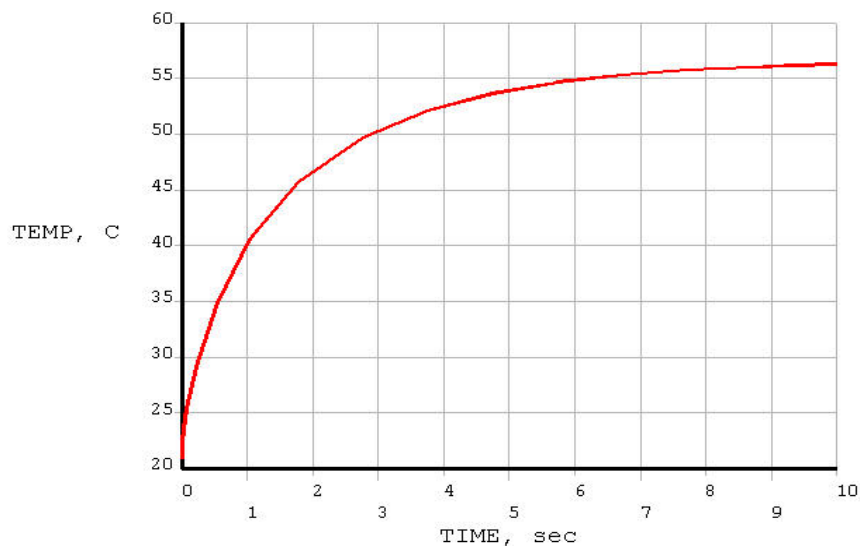


Figure 5: Temperature Equilibrium Plot at Node 7910

2. The first 5 cycles (1 second) are shown in figure 6.

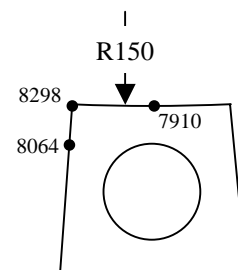
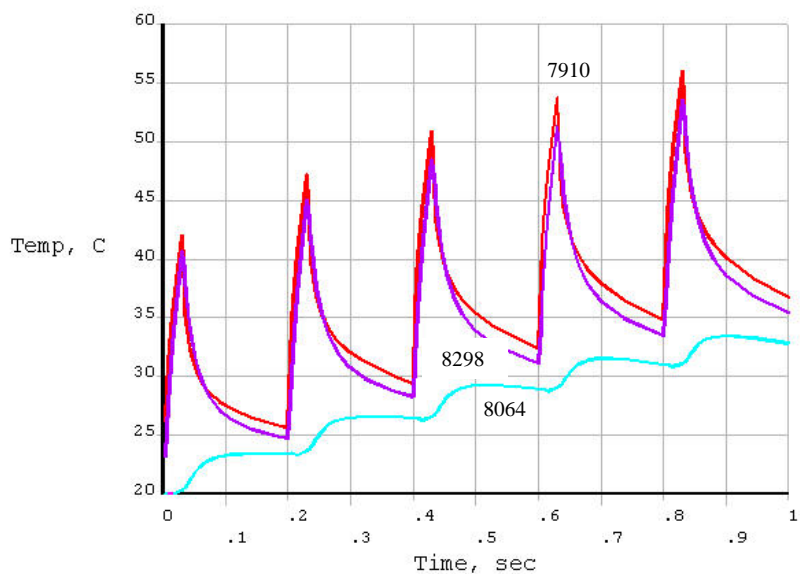


Figure 6: Temperature Cycling - Start of Pulsing

3. The temperature distribution of the EC at the end of the 30 mS pulse after LT cycling is shown in Figure 7. Figure 8, the temperature response plot, shows the temperature range between 52C and 73C.

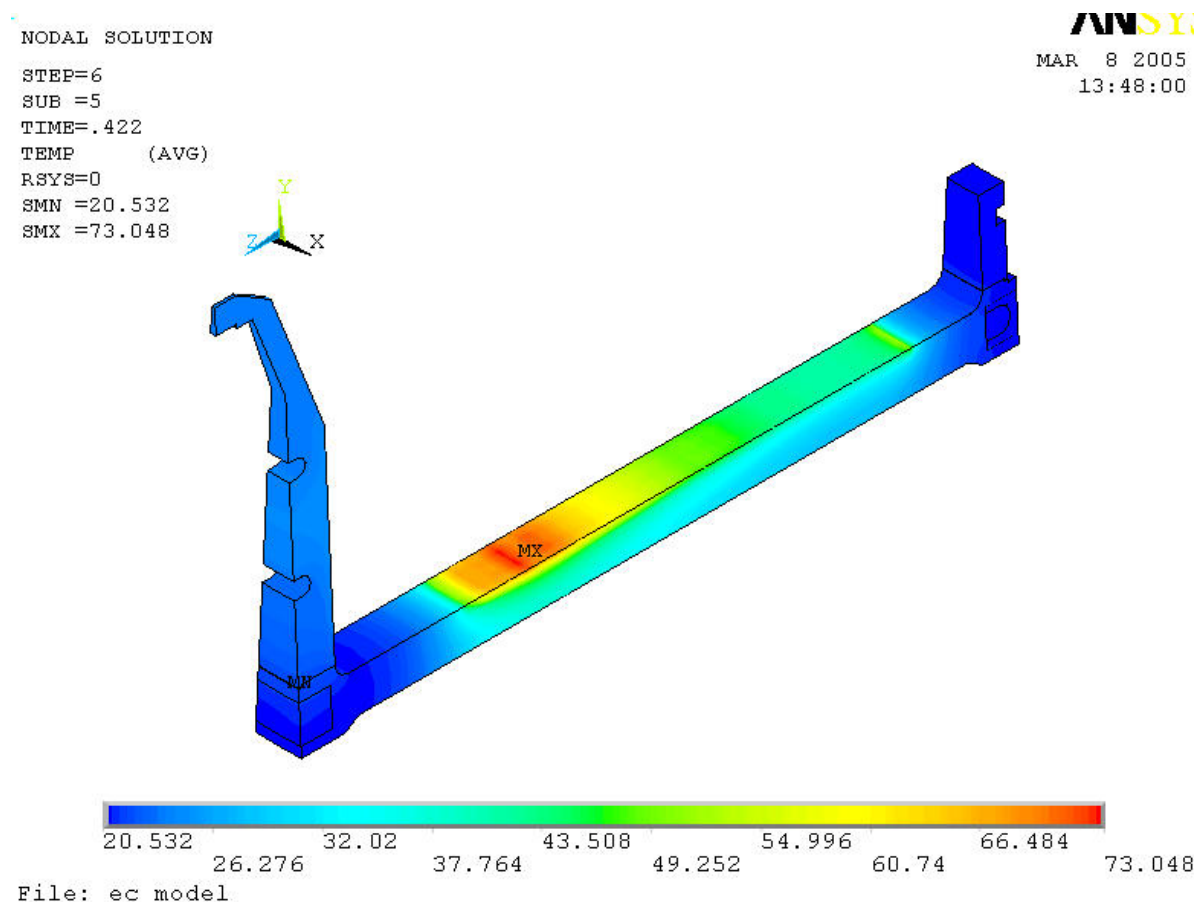


Figure 7: Temperature Distribution

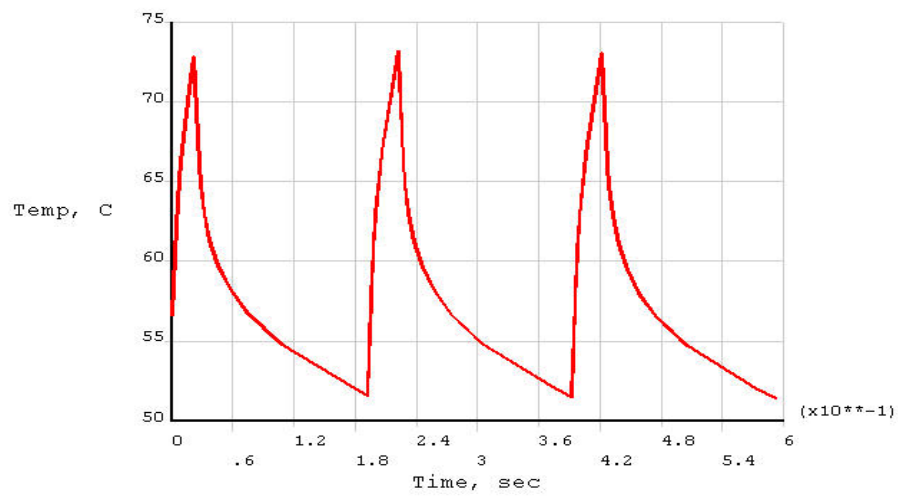


Figure 8: Time-Temperature (Node 7910)

4. The maximum heat flux into the cooling channel is $.457 \times 10^6$ watts/m² (.457 W/mm²) and it occurs 16mS after the end of the 30 mS pulsed beam. Figure 9 shows the radial heat flux in W/m² (negative is toward the center of the cooling channel). Figure 10 shows the time plot of the heat flux.

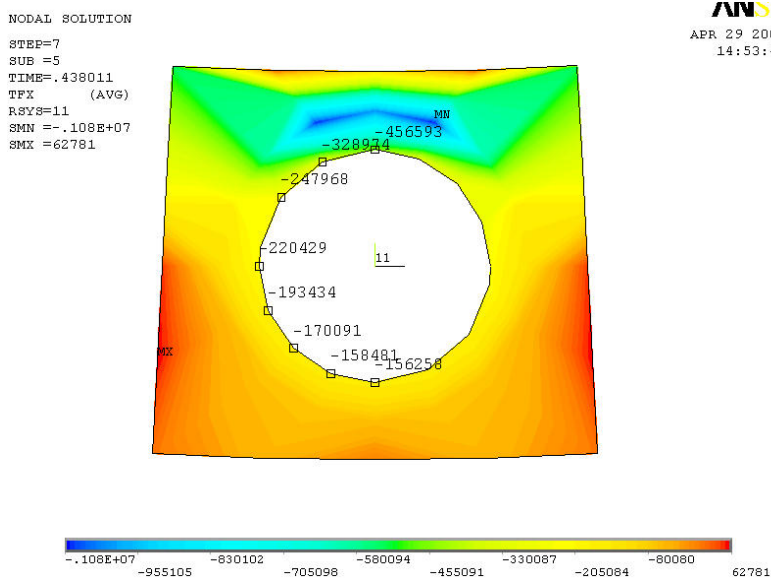
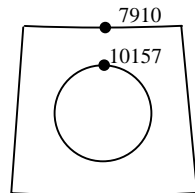
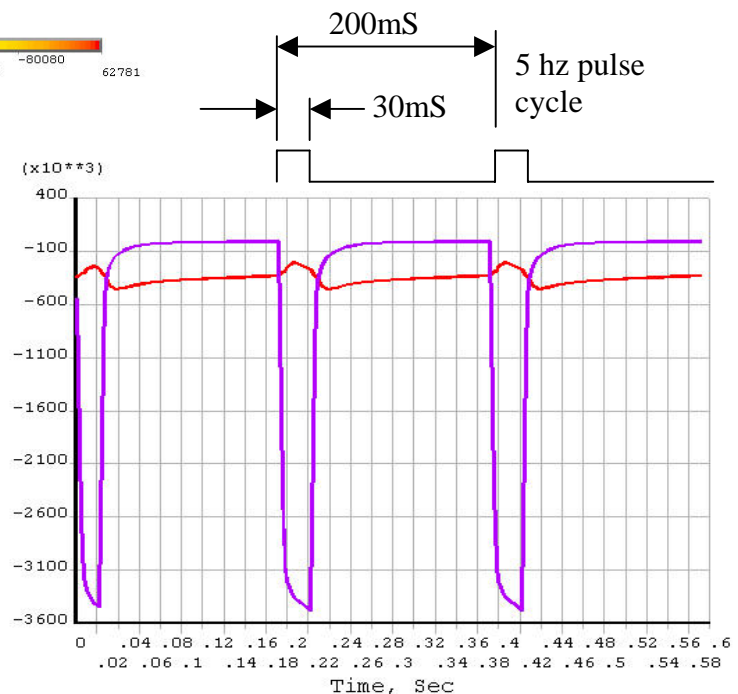


Figure 9: Heat Flux, X-dir (X-dir is toward center of channel)

Figure 10: Heat Flux at EC Inside Diameter (Node 7910) and at Channel (Red – Node 10157)



HFLUX, W/m2



Verification of Transient Thermal Response:

The following calculation estimates the temperature rise of beryllium copper subjected to a surface heat flux of 350 watts per cm² for 30mS to be 23C. The FE model result gives a temperature rise of 22.5C (See figure 6).

Estimate of Temperature Rise in Semi-infinite Solid with Heat Generation^{1,2}

k = conductivity, watt/m*C

c = specific heat, joule/kg*C

ρ = density, kg/m³

α = diffusivity, m²/sec

x = distance from incident surface, m

τ = time, sec

t_0 = initial surface temp.

ϕ_0 = heat flux at x = 0, watt/m²

$$k_{cu} := 242 \cdot \frac{\text{watt}}{\text{m} \cdot \text{degC}}$$

$$c_{cu} := 419 \cdot \frac{\text{joule}}{\text{kg} \cdot \text{degC}}$$

$$\rho_{cu} := 8830 \cdot \frac{\text{kg}}{\text{m}^3}$$

$$t_0 := 20 \cdot \text{degC} \quad x := 0 \cdot \text{m}$$

$$\phi_0 := 3.5 \cdot 10^6 \cdot \frac{\text{watt}}{\text{m}^2}$$

$$\tau := .03 \cdot \text{sec}$$

$$\alpha_{cu} := \frac{k_{cu}}{\rho_{cu} \cdot c_{cu}}$$

$$\alpha_{cu} = 6.541 \times 10^{-5} \text{ m}^2 \text{ sec}^{-1}$$

$$z := \frac{x}{\sqrt{4 \cdot \alpha_{cu} \cdot \tau}}$$

variable z

$$\text{erfz} := \frac{2}{\sqrt{\pi}} \cdot \int_0^z e^{-\beta^2} d\beta$$

error function, erf

$$\text{erfcz} := 1 - \text{erfz}$$

complementary error function, erfc

$$\text{ierfcz} := \frac{1}{\sqrt{\pi}} \cdot e^{-z^2} - z \cdot \text{erfcz}$$

integral complementary error function, ierfc

$$\Delta t := \left(\frac{\phi_0}{k_{cu}} \cdot \sqrt{4 \cdot \alpha_{cu} \cdot \tau} \cdot \text{ierfcz} \right)$$

$$\Delta t = 22.861 \text{ degC}$$

Part III. FE Model Structural Analysis

The cycling stress resulting from the pulse-induced temperature gradient is evaluated at two times:

1. In the early times when pulsing has just begun (fig 6).
2. After the EC has reached maximum temperature (fig 8).

The EC deflection is .1mm maximum in the axial direction.

Mean Stresses and Stress Ranges at Start of Pulsing:

Figure 11 shows the stress range at the maximum stress location on the inside diameter of the EC. The Von Mises stress here changes from about 5 ± 5 ksi to 14 ± 2 ksi in the first five cycles. The stresses on the outside diameter shown in figure 11 are considerably less.

Notes:

- e. The Von Mises stress is used as the failure criteria.
- f. The straight lines connecting the max and min points do not represent the actual stress-time histories, which are not linear.

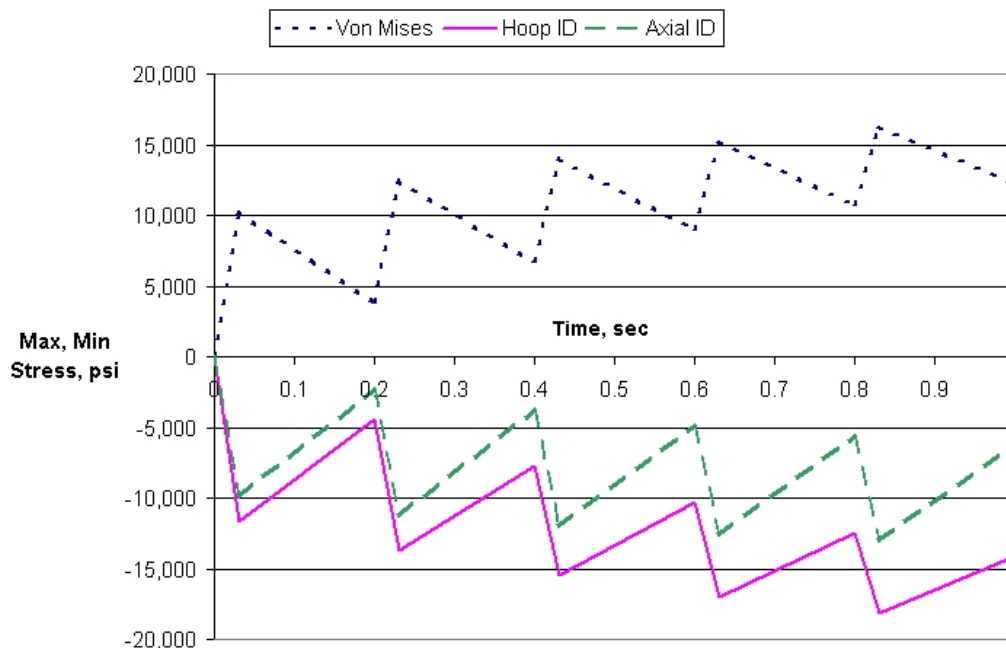


Figure 11: Maximum Stress on EC Inside Diameter

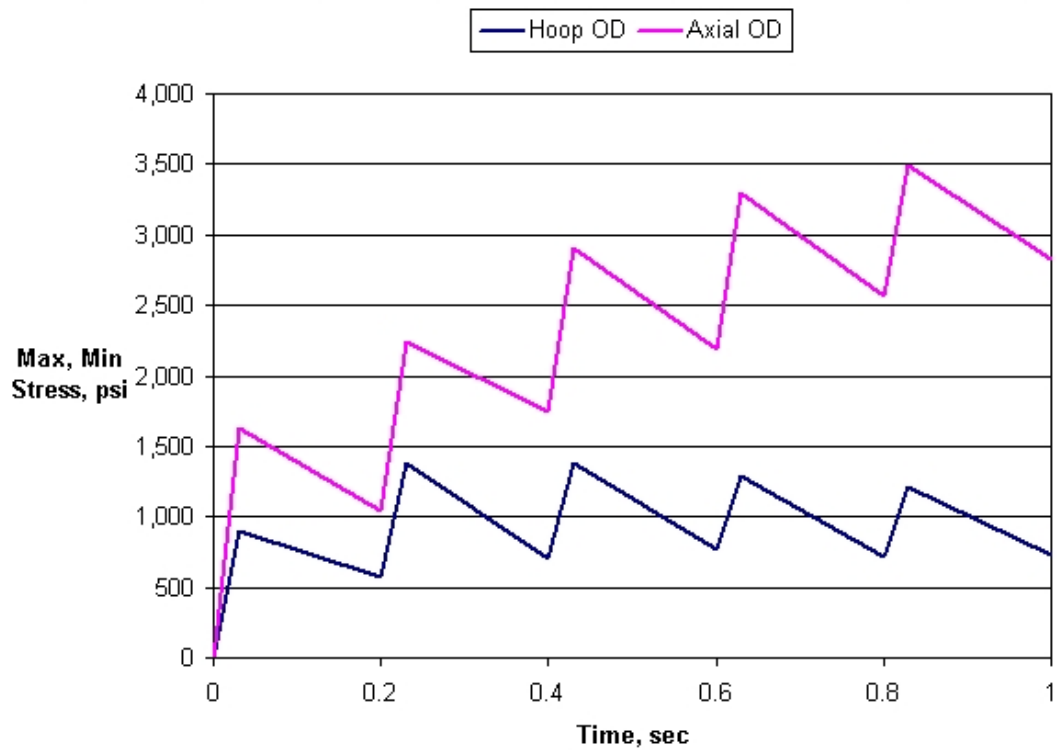


Figure 12: Maximum Stress on EC Outside Diameter

Mean Stresses and Stress Ranges at Steady Cycling:

The mean Von Mises stress at the maximum location (on ID) is 23.8 ksi with a stress range of .5 ksi (+/-.25ksi).

Load Step	Max. Stress Levels, ksi				
	Von Mises Stress	Hoop Stress		Axial (Z) Stress	
		Ten O.D.	Comp I.D.	Ten O.D.	Comp I.D.
End of Pulse	24.1	1.80	-27.4	4.73	-9.66
Start of Pulse	23.6	1.93	-27.3	5.58	-15.2

Figures 13, 14, and 15 show the stress contours at the end of the pulse. Stress levels are in Pascals ($1 \times 10^5 \text{ Pa} = 14.5 \text{ psi}$).

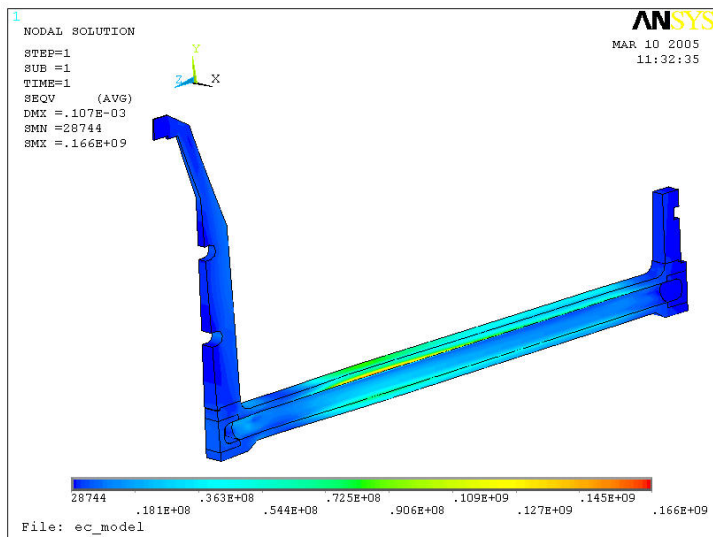


Figure 13: Von Mises Stress-End of 30 mS Pulse (24.1 ksi max, dropping to 23.6 ksi)

Figure 14: Tangent or Hoop Stress-End of Pulse (27.4 ksi I.D. compression, dropping to 27.3 ksi)

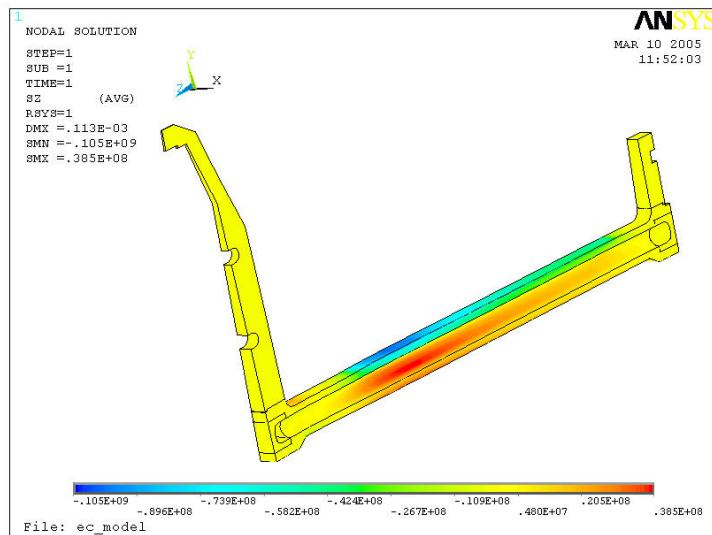
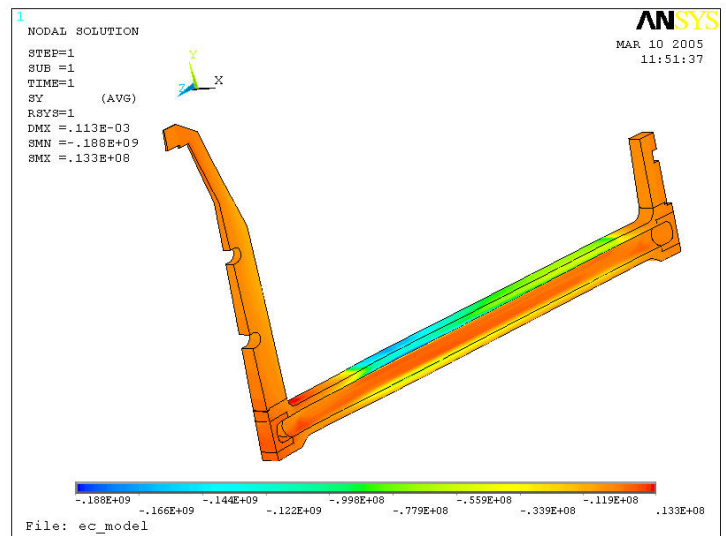


Figure 15: Axial Stress-End of Pulse (9.66 ksi I.D. compression, increasing to 15.2 ksi)

Summary:

The results of the FE model using beryllium copper, C17510, AT temper show that the stress levels are well below the yield strength. The maximum Von Mises stress occurs on the inside diameter of the EC and is 24 ksi, about 30% of the yield strength. The inside diameter stresses are compressive. The outside diameter, tensile stresses are much lower.

Part IV. Analysis of Fatigue Strength of Copper Alloys for EC

Considerations in Evaluating Fatigue Life:

Fatigue is a complex phenomenon resulting from microscopic crack propagation. Fatigue failures frequently result from material or manufacturing flaws. The calculation of fatigue life for the electron collector is an estimate for several reasons:

1. The documented fatigue strengths of materials are determined from cyclic axial tensile loading or reversed bending (i.e., rotating beam) fatigue tests, instead of thermal cycle loading.
2. Fatigue tests are performed under ideal conditions using carefully machined standard test specimens with polished surface finish.
3. Fatigue tests provide fatigue strength data based on fully reversed load cycles with a mean stress of zero. For non-zero mean stress the fatigue life is estimated by extrapolation methods, such as the Modified Goodman Diagram.
4. The EC will be constructed of a copper alloy material. Copper alloys do not have a defined endurance limit (i.e., stress level below which fatigue failure will never happen). The fatigue strength of copper alloys continues to decrease with increasing cycles, and fatigue failure will occur eventually regardless of how low the stress amplitude.

Note: Some metals have a definite endurance limit, such as ferrous and titanium alloys.

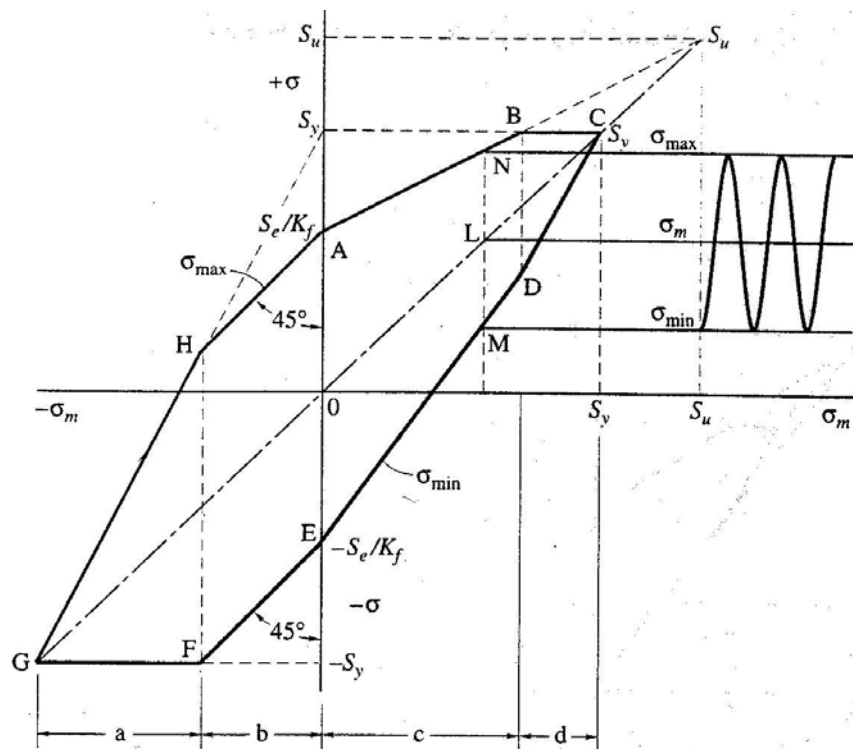
Procedure for evaluating fatigue:

1. Mean stress levels and stress ranges resulting from the thermal load cycle of the pulsed beam are calculated using FE methods.
2. Obtain fatigue strength of copper alloys that can be used in EC from manufacturer or published fatigue test results. Fatigue strength is the stress that will cause failure at a

given number of completely reversed stress cycles with a zero mean stress.

3. Calculate 'modified fatigue strength' to adjust the fatigue strength obtained in step 2 (idealized conditions) to reflect actual conditions. This takes into account the actual operating temperature⁶, actual surface finish of the part, and confidence level in the result.
4. Develop the Modified Goodman Diagram to determine fatigue strength at non-zero mean stress conditions. See Fig 7.10 below from Ref (3).
5. Evaluate suitability of copper alloy to be used in the EC by comparing the calculated 'in service' stresses (i.e., mean stresses and stress ranges) to the limits shown on the modified Goodman diagram.

Figure 7.10 Complete modified Goodman diagram, plotting stress as ordinate and mean stress as abscissa.



Conclusions:

The maximum stress calculated in Part III is 28,800 \pm 250 psi, occurring on the EC inside diameter. Fortunately, the higher stresses on the inside diameter are compressive and less susceptible to fatigue failure (shown by the higher permissible

stress range at the bottom compressive part of the Goodman diagram). The outside diameter stresses are tensile, and about 25% of the inside diameter stresses. The stress amplitudes resulting from the pulsed beam are very low, generally less than 3 ksi. This includes both the start of beam pulsing and steady cycling at maximum operating temperature. The Modified Goodman Diagram, Figure 16, developed in the following calculation indicates that these amplitudes will not cause fatigue failure up to 10^8 cycles. A few notes of caution are:

1. The material properties of the EC should not be degraded by vacuum furnace brazing, or must be restored after brazing.
2. The conductivity of the beryllium copper used in the EC should be certified. It would be preferable to use the Brush Wellman high purity grade, Hycon 3 HP⁵ since it has 75% of the conductivity of OFHC copper, further reducing stress levels.
3. Beryllium copper does not have a defined endurance limit. In theory the material will eventually fail as cycles are accumulated. While failure due to 10^8 cycles is not expected, this corresponds to only 16+ weeks of full time running. Since 10^8 cycles is considered infinite life in most applications, fatigue data beyond this may not be available.

Other methods to improve the durability of the EC may also be considered, such as better alloys, minimizing material or machining flaws, or surface work hardening techniques (e.g., shot peening).

Fatigue Calculation for Beryllium Copper

The Fatigue Calculations are based on the methods found in Ref. (3):

Strength, S'_f , of Materials: Beryllium Copper⁴, Alloy 3:

Fatigue Strength $S'_f := 38.0 \cdot 10^3 \cdot \text{psi}$
(10^8 cycles)

Yield Strength $S'_y := 80.0 \cdot 10^3 \cdot \text{psi}$

Ultimate Strength $S'_u := 100.0 \cdot 10^3 \cdot \text{psi}$

Calculation of Modified Fatigue Strength, S_f :

Fatigue Strength Modification Factors:

Fatigue Stress Concentration Factor, K_f $K_f := 1.0$

Surface Finish Factor, k_{sf} $k_{sf} := 4.51 \cdot \left(\frac{S'_u}{10^6 \cdot \text{Pa}} \right)^{-.265}$
-from Table 7.3, Ref (a) for 125 $\mu\text{-in}$
 $k_{sf} = 0.798$

*Size Factor, k_s $k_s := .6$

Reliability Factor, k_r $k_r := .9$
-from Table 7.4, Ref (a),
90% probability of survival

Temperature Factor, k_t $k_t := .92$
-from Ref (c)

Miscellaneous Factor, k_m $k_m := 1.0$

*Size factor takes into account the fatigue test specimen size compared to the size of the actual part. It takes into account the higher probability of more flaws being present in larger parts. The part size applies only in the area of high stress. Although estimated above, the size factor for the EC cannot be determined very accurately.

$$S_f := \frac{k_{sf} \cdot k_s \cdot k_r \cdot k_t \cdot k_m}{K_f} \cdot S'_f$$

$$S_f = 1.506 \times 10^4 \text{ psi}$$

Create Modified Goodman Diagram:

Make Modified Fatigue, Yield, and Ultimate Strengths Dimensionless for Plotting:

$$S_e := \frac{S_f}{10^3 \cdot \text{psi}}$$

$$S_e = 15.064$$

$$S_y := \frac{S'_y}{10^3 \cdot \text{psi}}$$

$$S_y = 80$$

$$S_u := \frac{S'_u}{10^3 \cdot \text{psi}}$$

$$S_u = 100$$

$$\sigma_{\max}(\sigma_m) := \begin{cases} (2 \cdot \sigma_m + S_y) & \text{if } -S_y \leq \sigma_m < (S_e - S_y) & \text{GH:} \\ (\sigma_m + S_e) & \text{if } S_e - S_y \leq \sigma_m < 0 & \text{HA:} \\ S_e + \sigma_m \cdot \left(1 - \frac{S_e}{S_u}\right) & \text{if } 0 \leq \sigma_m < \left(\frac{S_y - S_e}{1 - \frac{S_e}{S_u}}\right) & \text{AB:} \\ S_y & \text{if } \left(\frac{S_y - S_e}{1 - \frac{S_e}{S_u}}\right) \leq \sigma_m \leq S_y & \text{BC:} \end{cases}$$

$$\sigma_{\min}(\sigma_m) := \begin{cases} -S_y & \text{if } -S_y \leq \sigma_m < (S_e - S_y) & \text{FG:} \\ (\sigma_m - S_e) & \text{if } (S_e - S_y) \leq \sigma_m < 0 & \text{EF:} \\ \left(1 + \frac{S_e}{S_u}\right) \cdot \sigma_m - S_e & \text{if } 0 \leq \sigma_m < \left(\frac{S_y - S_e}{1 - \frac{S_e}{S_u}}\right) & \text{DE:} \\ (2 \cdot \sigma_m - S_y) & \text{if } \frac{S_y - S_e}{1 - \frac{S_e}{S_u}} \leq \sigma_m \leq S_y & \text{CD:} \end{cases}$$

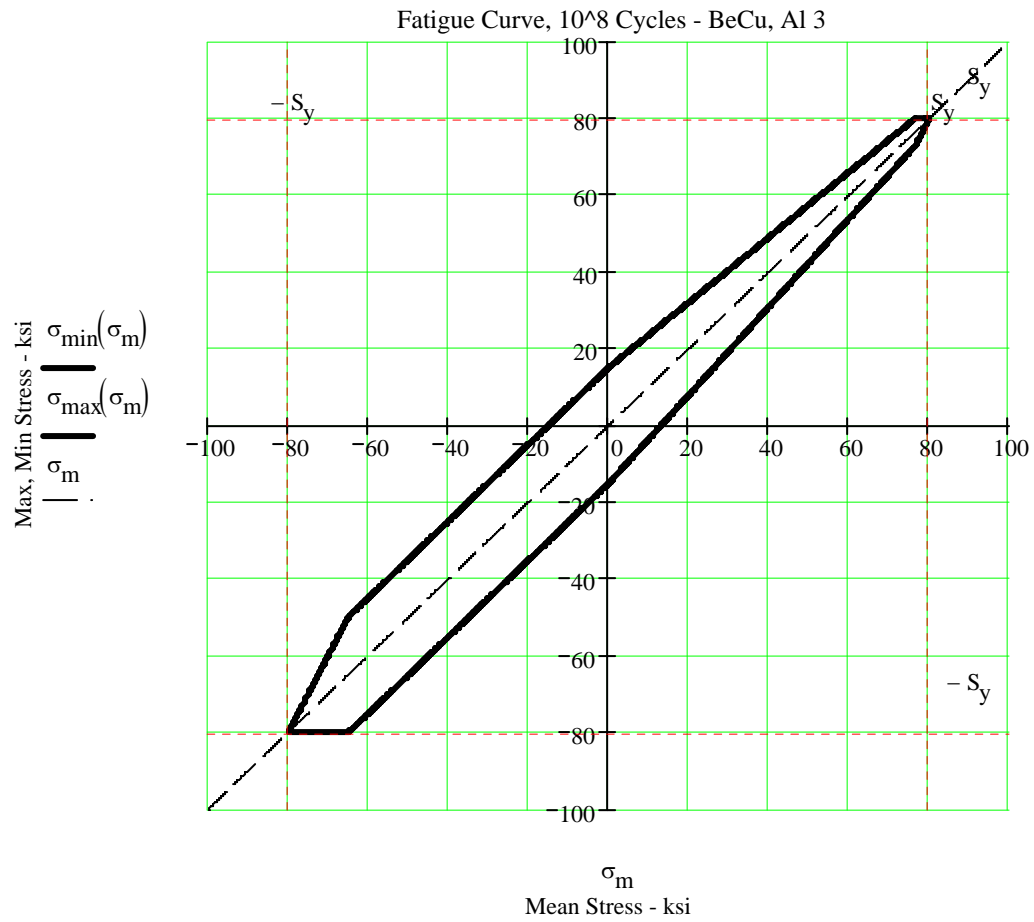


Figure 16: Modified Goodman Diagram for BeCu, C17510

Part V. Convective Heat Transfer In the EC⁶

Definition of Critical Heat Flux:

The thermal analysis of the water-cooled electron collector (EC) is conducted to evaluate the suitability of the electron collector for high heat loads. There are three possible modes of heat transfer that can occur in this electron collector, cooled by water much lower in temperature than saturation (i.e., subcooled): normal single-phase convective heat transfer, subcooled boiling, or DNB (departure from subcooled nucleate boiling). The first mode is defined by conventional forced heat convection methods. In the second mode subcooled boiling vapor bubbles form on the heated surface and condense in the cold water away from the tube wall. The bubbles grow and collapse while attached to or sliding along the heated surface. The process is sometimes accompanied by noise and vibration. When subcooled boiling becomes fully developed, heat transfer by the 'single phase forced convection process' no longer exists since a bubble layer replaces the film boundary layer. Interestingly, during fully developed boiling the surface temperature of the collector wall approaches a maximum value and is no longer significantly affected by the mass velocity and degree of subcooling (p. 188,197). The last condition, known as DNB, results in a severe drop in the local heat transfer coefficient at the channel wall due to the replacement of water by vapor, and may lead to failure. The heat flux that causes this condition is called the critical heat flux, or CHF.

There are two ways in which the critical heat flux condition can be reached: simply by a very high local heat flux and secondly by a lower heat flux and a longer exposure. The first case is similar to pool boiling, because the mass velocity does not significantly affect the CHF. In the latter case the water flows along a heated channel long enough for boiling, then phase change to gas (higher void fraction), followed by 'dryout' of the channel wall. In the electron collector, however, the water enters and leaves the short cooling channel in the subcooled condition. Due to the high degree of subcooling in the EC, saturated boiling and 2-phase flow do not occur.

CHF Factors in the EC:

Several empirical relationships (correlations) have been developed for calculating the critical heat flux of tubes that are heated uniformly axially and circumferentially. Although many of these methods are based on a local condition hypothesis that the critical heat flux is solely a function of the mass quality (or degree of subcooling) at the point of overheating, these relationships evaluate the critical heat flux as heat is added uniformly along the tube. The coolant gains energy as it flows through the channel, and the critical heat flux occurs at the channel exit. The use of independent variables of mass velocity, G , and distance along the heated tube, z , determines the degree of subcooling at the 'z' location of interest based on uniform heat into the tube. The application of these relationships to a tube that is non-uniformly heated circumferentially would result in an incorrect critical heat flux value.

Most empirical correlations have been developed for vertically oriented, straight tube applications. The EC flow passages are horizontal, serpentine flow passages. 'The difference in critical heat flux between horizontal and vertical tubes will decrease as the mass velocity and/or the system pressure is increased and the tube diameter is decreased'⁶(p. 365). Since the mass velocity in the EC is very high, these methods are considered suitable for use. The serpentine flow path (i.e., flow turns) has been noted to have an adverse effect on the critical heat flux in two phase, low mass velocity applications due to stratification and dry-out. It is considered less of a concern in the EC, since saturated boiling does not occur in the highly subcooled water.

Operating Parameters of the EC:

The parameters used in the calculations for the electron collector are as follows:

1. The electron collector inside diameter is 300 mm and the length is about 248 mm. The water passes through 9 mm drilled passages in the 15 mm thick collector wall.
2. There are 10 cooling loops in the collector wall; each loop consisting of 6 serpentine passes for a total length of 1.5 meters.
3. The total heat dissipated by the electron collector is 300 kW during a 30mS, 5 hz pulse for an average of 45 kW, a duty factor of .15.
4. The water enters the cooling channel at 30C, 122C subcooled below the saturation temperature at the inlet pressure of 5 bar. There is a 4C temperature rise of the water through the cooling loop at a flow rate of 4 gpm (15 lpm), so it exits at 34C at about 2.6 bar), which is 95C subcooled.
5. The calculations were based on an overly severe 3.5 W/mm² peak heat flux impinging uniformly on the inner collector surface (the actual varying distribution is shown in Figure 3). The FE model determined the variable heat flux distribution around the cooling channel circumference, shown in Figure 9. The maximum heat flux reaching the water channel was found to be only about .46 W/mm² about 16 mS after the end of the pulse.
6. The overall heat transfer coefficient between the cooling water and the EC cooling channel with 30C inlet water temperature is calculated to be 13,800 watts/m²-C.

Summary of the Heat Transfer Calculations:

Electron Collector Cooling:

The temperature of the water and the temperature of the cooling channel wall along the flow path, z , is approximately shown in Figure 17. The plot shows the water temperature, the average wall temperature, and the wall temperature on the hot side along the flow direction, z . The inlet and outlet water conditions are highly subcooled and boiling does not occur in the 1.5 meter long flow channel of the EC. The differential temperature between the water and the hot side of the channel wall, based on single phase convective heat transfer, is calculated to be 33 C. A possible benefit of operating with boiling is that the EC wall temperature stops increasing at the point where boiling starts, z_{onb} (onb—onset of nucleate boiling). Also, the heat transfer rate increases substantially during boiling. During partial subcooled boiling the heat transfer mechanism is defined by a combination of single-phase convection and subcooled boiling. During fully developed subcooled boiling, the differential temperature between the water and the hot side channel wall will reach a maximum of 19C. A reduction in the maximum temperature is an important factor in the minimization of stress levels causing material fatigue failure. The concern with boiling is that the collector may come closer to operating at the critical heat flux.

Critical Heat Flux (CHF):

The Bowring and Biasi Correlations were used to calculate the heat flux at which surface temperatures rise sharply, possibly causing rupture or melting. In order to avoid the misapplication of the maximum heat flux to a formula designed for uniform heating, the Bowring calculation was made at ' $z=0$ ', the beginning of the flow channel, using the subcooled conditions found at the exit. The Biasi calculation is based on pressure only. The operating parameters of the EC fall within the data range that the Bowring and Biasi Correlations were empirically developed from, except for the flow channel length used here ($z=0$). As a comparison the

critical heat flux for Pool Boiling (Zuber) is provided, since mass velocity is not a factor in full boiling⁶.

Critical Heat Flux, $N \times 10^6$ watts/m ²			
<u>Pressure, bar</u>	<u>Bowring</u>	<u>Biasi</u>	<u>Pool Boiling</u>
1	3.6	2.9	4.9
2	4.4	3.5	
5	6.4	4.6	
17	11.2	7.2	
20	12.1	7.5	14.5

The maximum heat flux expected in the EC is about $.46 \times 10^6$ watts/m² resulting from the short 30mS pulse. This is a conservative margin compared to the CHF values above at a water pressure of 2 bar.

Other CHF Research:

Experiments by Boyd⁹ provided results of CHF testing of steady state subcooled flow boiling in uniformly heated, horizontal circular channels. An example of the results is given as a comparison to the data above:

	<u>Electron Collector</u>	<u>Boyd</u>
Exit Pressure, bar	5	4.5
Tube Diameter, mm	9	10.2
Tube Length, cm	0*	49
Mass Velocity, Mg/m ² -s	4.0	4.0
Inlet Temperature, C	20	30
Inlet Subcooling, C	126	122
CHF, W/cm ²	640 above	700

*z=0 is used in the Bowring Correlation, and the exit conditions applied directly (See Calc below). The channel length of the EC is 150 cm.

Calculations of Convective Heat Transfer in EC:

The calculation methods are in accordance with Reference (6). These methods are for uniformly heated tubes, both circumferentially and along the flow direction. The calculations below have been adjusted to reflect non-uniform circumferential heat flux.

Flow Conditions:

Inlet Bulk Temperature: $T_{fi} := 303\text{ K}$ bar := 14.50377psi

Inlet Pressure, abs: $P_i := 72\text{ psi}$ $P_i = 5\text{ bar}$

Outlet Pressure, abs: $P_o := 38\text{ psi}$ $P_o = 2.6\text{ bar}$

*Sat Temp In @ P_i : $T_{isat} := 425\text{ K}$ (lookup)

*Sat Temp Out @ P_o : $T_{osat} := 402\text{ K}$ (lookup)

Sat Temp at 1 atm: $T_{atm.sat} := 373\text{ K}$

Subcooling of Water, (ΔT_{sub}), is the saturation temperature of water at system pressure, T_{sat} minus the actual water temperature, T_{fi} .
 $\Delta T_{subi} := T_{isat} - T_{fi}$
 $\Delta T_{subi} = 122\text{ K}$

Design Parameters:

Diameter of Channel $D := 9\text{ mm}$

Channel length $L := 1.5\text{ m}$

Volumetric Flow, V $V := 4 \frac{\text{gal}}{\text{min}}$ $V = 2.5 \times 10^{-4} \frac{\text{m}^3}{\text{s}}$

Channel Area $A := .785 D^2$
 $A = 6.4 \times 10^{-5} \text{ m}^2$

Velocity $v := \frac{V}{A}$ $v = 4 \text{ ms}^{-1}$

*Density, Inlet, @ T_{fi} $\rho_{fi} := 995 \frac{\text{kg}}{\text{m}^3}$ (lookup)

*Viscosity, Abs, @ T_{fi} $\mu_i := 798 \cdot 10^{-6} \frac{\text{N}\cdot\text{s}}{\text{m}^2}$ (lookup)

*Conductivity, @ T_{fi} $k_i := .623 \frac{\text{watt}}{\text{m}\cdot\text{K}}$ (lookup)

*Specific Heat, @ T_{fi} $c_{pi} := 4.177 \frac{\text{joule}}{\text{gm}\cdot\text{K}}$ (lookup)

Mass Velocity: $G := \rho_{fi} \cdot v$ $G = 3.95 \times 10^3 \text{ kg m}^{-2} \text{ s}^{-1}$

EC Collector Heat Load:

Heat Transfer Area for Single Cooling Channel	$A_c := \pi \cdot D \cdot L$	$A_c = 0.042 \text{ m}^2$
Electron Collector Total Heat Load	$Q_{ec} := 45 \cdot \text{kW}$	
No. of Cooling Channels	$n := 10$	
Heat Flux at Cooling Channel, Average	$\phi_{av} := \frac{Q_{ec}}{n \cdot A_c}$	$\phi_{av} = 1.1 \times 10^5 \frac{\text{watt}}{\text{m}^2}$
Max Heat Flux from FE Model	$\phi_h := .456 \cdot 10^6 \cdot \frac{\text{watt}}{\text{m}^2}$	
Non Uniformity, ϕ_h/ϕ_{av}	$\frac{\phi_h}{\phi_{av}} = 4.3$	

Calculate Reynolds No and Prandtl No:

$$N_{re} := \frac{\rho_{fi} \cdot D \cdot v}{\mu_i} \quad N_{pr} := \frac{\mu_i \cdot c_{pi}}{k_i}$$
$$N_{re} = 4.5 \times 10^4 \quad N_{pr} = 5.4$$

Calculate Overall Heat Transfer Coefficient:

Nusselt Number: $N_{nu} := .023 N_{re}^{.8} \cdot N_{pr}^{.3} \quad (5.7)$

$$N_{nu} = 199.2$$

Overall Heat Transfer Coefficient in non-boiling region, h_o

$$h_o := \frac{k_i}{D} \cdot N_{nu}$$
$$h_o = 13.8 \frac{\text{kW}}{\text{m}^2 \cdot \text{K}}$$

Using Seider & Tate Eqn for high ΔT , μ_s is viscosity at surface for $T_s = 107 \text{ F}$.

$$\mu_s := 744 \cdot 10^{-6} \cdot \frac{\text{N} \cdot \text{s}}{\text{m}^2}$$

$$N_{pr2} := 4.16$$

$$N_{nu2} := .027 \cdot N_{re}^{.8} \cdot N_{pr2}^{.33} \cdot \left(\frac{\mu_i}{\mu_s} \right)^{.14}$$

$$N_{nu2} = 228.5$$

Calculate Water Temperature at Exit of Cooling Channel, $z=L$:

$$T_{fL} := T_{fi} + \frac{4 \cdot \phi_{av} \cdot L}{G \cdot c_{pi} \cdot D} \quad (5.2)$$

$$T_{fL} = 307.3 \text{ K}$$

Calculate Water Subcooling at z=L:

$$\Delta T_{\text{subL}} := T_{\text{osat}} - T_{\text{fL}}$$

$$\Delta T_{\text{subL}} = 94.7\text{K}$$

Calculate ΔT_{fh} between the bulk water temperature and tube wall (hot side) in single phase convective region, and **ΔT_{fav}** between the water and average tube wall temperature.

$$\Delta T_{\text{fh}} := \frac{\phi_{\text{h}}}{h_{\text{o}}} \quad \Delta T_{\text{fav}} := \frac{\phi_{\text{av}}}{h_{\text{o}}}$$

$$\Delta T_{\text{fh}} = 33.1\text{K} \quad \Delta T_{\text{fav}} = 7.7\text{K}$$

Calculate z_{sc} , distance z from flow entrance that subcooled conditions exist:

$$z_{\text{sc}} := \frac{G \cdot c_{\text{pi}} \cdot D}{4 \cdot \phi_{\text{av}}} \cdot (T_{\text{osat}} - T_{\text{fi}}) \quad (5.3)$$

$$z_{\text{sc}} = 34.6\text{m}$$

Since z_{sc} is greater than the cooling channel length, the average (bulk) water condition is subcooled along the channel.

Calculate z' at $T_{\text{w}}=T_{\text{isat}}$, the distance z from the flow entrance where the average tube wall temperature equals the water saturation temperature:

(Eqn 5.9, $\Delta T_{\text{sat.onb}}=0$)

$$z' := \frac{G \cdot c_{\text{pi}} \cdot D}{4} \cdot \left(\frac{\Delta T_{\text{subL}}}{\phi_{\text{av}}} - \frac{1}{h_{\text{o}}} \right)$$

$$z' = 30.4\text{m}$$

Calculate $\Delta T_{\text{sat.onb}}$, Wall Temperature above Water Saturation Temperature at Onset of Nucleate Boiling.

w/ Average Heat Flux (Eqn 5.23)

$$\Delta T_{\text{sat.onb}} := .556 \text{ K} \cdot \left[\frac{\left(\frac{\phi_{\text{av}}}{\frac{\text{watt}}{\text{m}^2}} \right)}{1082 \left(\frac{P_{\text{i}}}{\text{bar}} \right)^{1.156}} \right]^{.463} \cdot \left(\frac{P_{\text{o}}}{\text{bar}} \right)^{.0234}$$

$$\Delta T_{\text{sat.onb}} = 2 \text{ K}$$

w/ Hot Side Heat Flux

$$\Delta T_{\text{sat.onbh}} := .556 \text{ K} \cdot \left[\frac{\left(\frac{\phi_{\text{h}}}{\frac{\text{watt}}{\text{m}^2}} \right)}{1082 \left(\frac{P_{\text{i}}}{\text{bar}} \right)^{1.156}} \right]^{.463} \cdot \left(\frac{P_{\text{o}}}{\text{bar}} \right)^{.0234}$$

$$\Delta T_{\text{sat.onbh}} = 4 \text{ K}$$

Calculate the Tw max at Fully Developed Subcooled Boiling. (ΔT_{sat}), tube wall temperature above the water saturation temperature in the subcooled boiling region, using Jens and Lottes relationship.

w/ Average Heat Flux Eqn (5.50)

$$\Delta T_{\text{sat}} := 25 \cdot \text{K} \cdot \left(\frac{\phi_{\text{av}}}{10^6 \cdot \frac{\text{watt}}{\text{m}^2}} \right)^{.25} \cdot e^{\frac{-P_o}{62 \cdot \text{bar}}}$$

$$\Delta T_{\text{sat}} = 13.7\text{K}$$

$$T_{\text{wmax}} := \Delta T_{\text{sat.h}} + T_{\text{osat}}$$

$$T_{\text{wmax}} = 421.7\text{K}$$

w/ Hot Side Heat Flux

$$\Delta T_{\text{sat.h}} := 25 \cdot \text{K} \cdot \left(\frac{\phi_{\text{h}}}{10^6 \cdot \frac{\text{watt}}{\text{m}^2}} \right)^{.25} \cdot e^{\frac{-P_o}{62 \cdot \text{bar}}}$$

$$\Delta T_{\text{sat.h}} = 19.7\text{K}$$

Calculate Onset of Nucleate Boiling, z_{onb} , distance z from flow entrance to the onset of nucleate boiling and **z_{onbh}** to onset on hot side of cooling channel.

Water temps at same locations, **T_{fonb}** and **T_{fonbh}** , respectively.

w/ Average Heat Flux

(5.9, similar to 5.16)

$$z_{\text{onb}} := \frac{G \cdot c_{\text{pi}} \cdot D}{4} \cdot \left(\frac{\Delta T_{\text{subL}} + \Delta T_{\text{sat.onb}}}{\phi_{\text{av}}} - \frac{1}{h_o} \right)$$

$$z_{\text{onb}} = 31.1\text{m}$$

$$T_{\text{fonb}} := T_{\text{fi}} + \frac{4 \cdot \phi_{\text{av}} \cdot z_{\text{onb}}}{G \cdot c_{\text{pi}} \cdot D}$$

$$T_{\text{fonb}} = 392\text{K}$$

w/ Heat Flux - Hot Side

$$T_{\text{wnb}} := T_{\text{osat}} + \Delta T_{\text{sat.onbh}}$$

$$z_{\text{onbh}} := \frac{G \cdot c_{\text{pi}} \cdot D}{4 \cdot \phi_{\text{av}}} \cdot \left(T_{\text{wnb}} - T_{\text{fi}} - \frac{\phi_{\text{h}}}{h_o} \right)$$

$$z_{\text{onbh}} = 24.5\text{m}$$

$$T_{\text{fonbh}} := T_{\text{fi}} + \frac{4 \cdot \phi_{\text{av}} \cdot z_{\text{onbh}}}{G \cdot c_{\text{pi}} \cdot D}$$

$$T_{\text{fonbh}} = 373\text{K}$$

Maximum Length of Cooling Channel, L_p , due to high pressure drop limit:

Pressure Loss per Channel Length, h_L

$$h_L := \frac{34 \cdot \text{psi}}{1.7 \cdot \text{m}} \quad h_L = 20 \frac{\text{psi}}{\text{m}}$$

Water Supply Pressure (gage), p

$$p_5 := 5 \cdot 14.5 \text{ psi} - 14.7 \text{ psi} \quad p_5 = 57.8 \text{ psi}$$

$$p_{20} := 20 \cdot 14.5 \text{ psi} - 14.7 \text{ psi} \quad p_{20} = 275.3 \text{ psi}$$

Maximum Channel Length, L_p , at 5 bar
and at 20 bar

$$L_5 := \frac{p_5}{h_L}$$

$$L_{20} := \frac{p_{20}}{h_L}$$

$$L_5 = 2.9\text{m}$$

$$L_{20} = 13.8\text{m}$$

Define Graph Parameters:

$$Z := \begin{pmatrix} 0\text{-m} \\ L \\ z_{\text{onbh}} \\ z_{\text{onb}} \\ z_{\text{sc}} \\ 50\text{-m} \end{pmatrix} \quad T_f := \begin{pmatrix} T_{\text{fi}} \\ T_{\text{fL}} \\ T_{\text{fonbh}} \\ T_{\text{fonb}} \\ T_{\text{osat}} \\ T_{\text{osat}} \end{pmatrix} \quad T_w := \begin{pmatrix} T_{\text{fi}} + \Delta T_{\text{fav}} \\ T_{\text{fL}} + \Delta T_{\text{fav}} \\ T_{\text{fonbh}} + \Delta T_{\text{fav}} \\ T_{\text{osat}} + \Delta T_{\text{sat.onb}} \\ T_{\text{osat}} + \Delta T_{\text{sat}} \\ T_{\text{osat}} + \Delta T_{\text{sat}} \end{pmatrix} \quad T_{\text{wh}} := \begin{pmatrix} T_{\text{fi}} + \Delta T_{\text{fh}} \\ T_{\text{fL}} + \Delta T_{\text{fh}} \\ T_{\text{osat}} + \Delta T_{\text{sat.onbh}} \\ T_{\text{osat}} + \Delta T_{\text{sat.h}} \\ T_{\text{osat}} + \Delta T_{\text{sat.h}} \\ T_{\text{osat}} + \Delta T_{\text{sat.h}} \end{pmatrix}$$

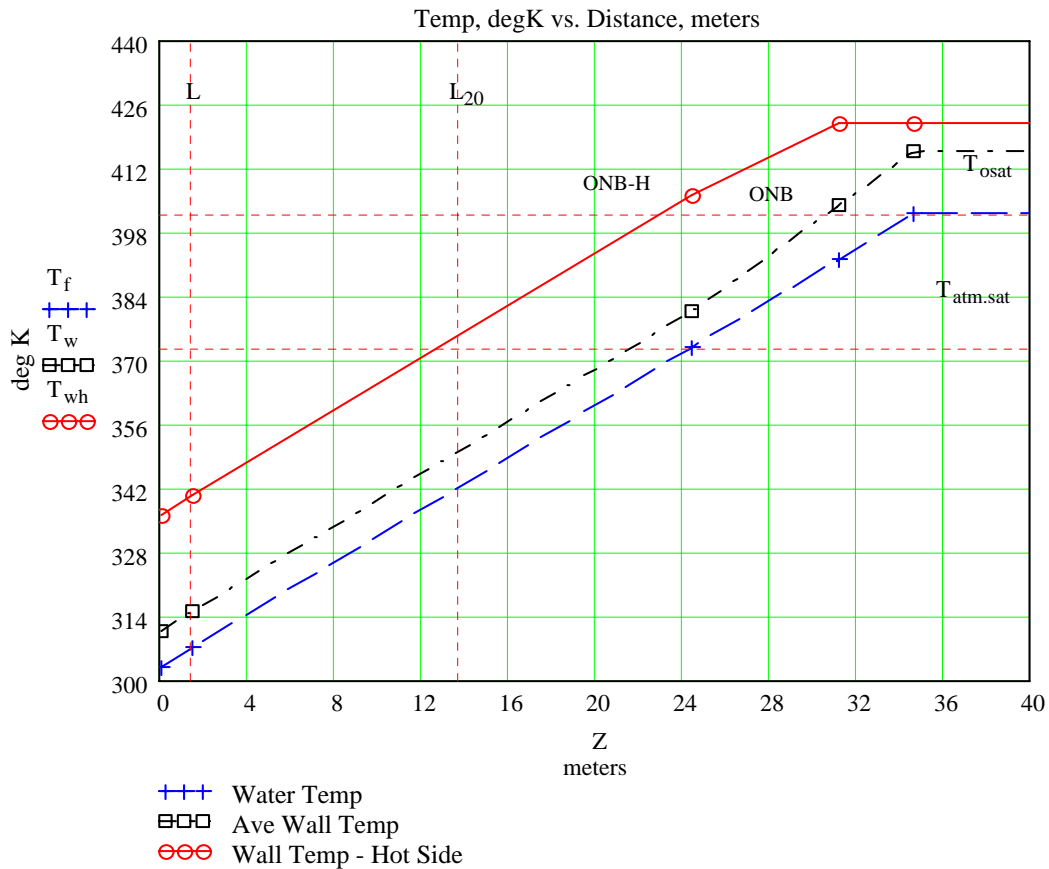


Figure 17: EC Water/Wall Temperature Profile

Note: The pressure drop beyond the flow channel length is not reflected in the water and channel wall temperature profiles above.

Calculation of the Critical Heat Flux using Bowring Correlation:

Several empirical correlations have been developed for calculating the Critical Heat Flux of uniformly heated tubes. Most of these methods suggest a local condition hypothesis that the critical heat flux is solely a function of the mass quality at the point of overheating, such as the MacBeth-Barnett and, Bowring correlations (Biasi does not). The use of independent variables of mass velocity, G and distance along the heated tube, z determines the degree of subcooling at the 'z' location of interest based on uniform heat into the tube. The application of these relationships to a non-uniformly heated tube would result in a lower critical heat flux value. In order to take into account the non-uniformity of heating, z is set to '0', and the maximum heat flux (not average) is applied to the water conditions existing at the outlet.

Data range of Bowring:	pressure	2-190 bar	$\frac{EC}{2-20}$
	tube dia	2-45 mm	9
	tube length	.15-3.7 m	1.7
	mass velocity	136-18600 kg/m ² -s	4000

Flow Conditions:

*Inlet Bulk Temperature:	$T_{fi} = 303K$	
*Inlet Pressure:	$P_i = 72\text{psi}$	$P_i = 5\text{bar}$
*Outlet Pressure:	$P_o = 38\text{psi}$	$P_o = 2.6\text{bar}$
*Sat Temp In @ P_i :	$T_{isat} = 425K$	
*Sat Temp Out @ P_o :	$T_{osat} = 402K$	
* Previously defined		

Determine Bowring Parameters F1, F2, F3, F4 from Table 8.4, p. 354 at Various Pressures P=1,2,5,17,20 bar:

Pressure, p:	$p := \begin{pmatrix} 1 \\ 2 \\ 5 \\ 17 \\ 20 \end{pmatrix}$
Bowring Parameters: F1,F2,F3,F4	
Enthalpy, i	
ifs = liquid enthalpy at 'p' and sat temp	
ifg = heat of vaporization at 'p'	

At inlet system pressure:					
	1 bar	2 bar	5 bar	17bar	20 bar
Bowring Parameters	$F1_1 := .478$	$F1_2 := .478$	$F1_3 := .478$	$F1_4 := .478$	$F1_5 := .478$
	$F2_1 := 1.782$	$F2_2 := 1.591$	$F2_3 := 1.019$	$F2_4 := .485$	$F2_5 := .441$
	$F3_1 := .4$	$F3_2 := .4$	$F3_3 := .4$	$F3_4 := .4$	$F3_5 := .4$
	$F4_1 := .0004$	$F4_2 := .0016$	$F4_3 := .0052$	$F4_4 := .0402$	$F4_5 := .0521$

Enthalpy i, fs-liquid saturated, fg-heat of vapor.

$$\begin{array}{lllll} \text{ifs}_1 := 419.1 \frac{\text{joule}}{\text{gm}} & \text{ifs}_2 := 503.7 \frac{\text{joule}}{\text{gm}} & \text{ifs}_3 := 635 \frac{\text{joule}}{\text{gm}} & \text{ifs}_4 := 871 \frac{\text{joule}}{\text{gm}} & \text{ifs}_5 := 908 \frac{\text{joule}}{\text{gm}} \\ \text{ifg}_1 := 2257 \frac{\text{joule}}{\text{gm}} & \text{ifg}_2 := 2202 \frac{\text{joule}}{\text{gm}} & \text{ifg}_3 := 2115 \frac{\text{joule}}{\text{gm}} & \text{ifg}_4 := 1924 \frac{\text{joule}}{\text{gm}} & \text{ifg}_5 := 1891 \frac{\text{joule}}{\text{gm}} \end{array}$$

Water Subcooling:

By Temperature: Subcooling of Water, ΔT_{sub} , is the sat temp of water, T_{sat} , at system pressure minus the actual water temp, T_f .

@ EC inlet temp $\Delta T_{\text{subi}} = 122\text{K}$ (previously defined)

@ EC outlet temp $\Delta T_{\text{subL}} = 94.7\text{K}$ (previously defined)

By Enthalpy: The subcooling is the saturated liquid enthalpy at the system pressure, ifs , minus the enthalpy of water at the actual conditions, i_f ($\sim i_f$ @ sat temp = actual water temp, p negl effect).

@ inlet	$i_{fi} := 125.7 \frac{\text{joule}}{\text{gm}}$	$\Delta i_{\text{subi}} := \text{ifs} - i_{fi}$	$\Delta i_{\text{subi}} = \begin{pmatrix} 293.4 \\ 378 \\ 509.3 \\ 745.3 \\ 782.3 \end{pmatrix} \frac{\text{joule}}{\text{gm}}$
@ outlet	$i_{fo} := 217 \frac{\text{joule}}{\text{gm}}$	$\Delta i_{\text{subo}} := \text{ifs} - i_{fo}$	$\Delta i_{\text{subo}} = \begin{pmatrix} 202.1 \\ 286.7 \\ 418 \\ 654 \\ 691 \end{pmatrix} \frac{\text{joule}}{\text{gm}}$

$$n := 2.0 - .00725p \quad (8.25) \quad n = \begin{pmatrix} 1.993 \\ 1.986 \\ 1.964 \\ 1.877 \\ 1.855 \end{pmatrix}$$

$$\overline{A} := \frac{2.317 \cdot \left(\frac{D \cdot G \cdot \text{ifg}}{4} \right) \cdot \left(\frac{\text{m} \cdot \text{s}}{\text{joule}} \right) \cdot F1}{1.0 + .0143 F2 \cdot D^{.5} \cdot \left(\frac{1}{\text{m}^{.5}} \right) \cdot G \cdot \left(\frac{\text{s} \cdot \text{m}^2}{\text{kg}} \right)} \quad (8..24) \quad \overline{C} := \frac{.077 \cdot F3 \cdot D \cdot G \cdot \left(\frac{\text{m} \cdot \text{s}}{\text{kg}} \right)}{1.0 + .347 F4 \cdot \left[\frac{G \cdot \left(\frac{\text{m}^2 \cdot \text{s}}{\text{kg}} \right)}{1356} \right]^n} \quad (8..24)$$

$$A = \begin{pmatrix} 2.1 \times 10^6 \\ 2.3 \times 10^6 \\ 3.2 \times 10^6 \\ 5.3 \times 10^6 \\ 5.5 \times 10^6 \end{pmatrix} \quad C = \begin{pmatrix} 1.09 \\ 1.09 \\ 1.08 \\ 0.99 \\ 0.97 \end{pmatrix}$$

The critical heat flux at $z_0=0$ determines the local critical heat flux at a known subcooled condition. The water condition at the outlet is applied directly, instead of allowing the formula to calculate the lower subcooling as the water flows along the tube.

$$\phi_{\text{crBow}} := \frac{A + \frac{D \cdot G \cdot \Delta i_{\text{subo}} \cdot \left(\frac{\text{m} \cdot \text{s}}{\text{joule}} \right)}{4}}{C + z_0 \cdot \frac{1}{\text{m}}} \quad z_0 := 0 \cdot \text{m}$$

$$\phi_{\text{crBow}} = \frac{\text{N} \times 10^6}{\begin{pmatrix} 3.57 \times 10^6 \\ 4.43 \times 10^6 \\ 6.43 \times 10^6 \\ 1.12 \times 10^7 \\ 1.21 \times 10^7 \end{pmatrix}} \quad \text{Watt/m}^2 \text{ or 'N' watts/mm}^2 \text{ at p1, p2, p3, p4} \quad p = \begin{pmatrix} 1 \\ 2 \\ 5 \\ 17 \\ 20 \end{pmatrix}$$

Calculation of the Critical Heat Flux using Biasi Correlation based on Quality at Outlet:

Subcooling defined Fluid Quality = $(i_z - i_{fs}) / i_{fg}$ (negative value denotes subcooled condition):
By Quality, X

$$\text{Inlet Condition: } X_i := \frac{\overrightarrow{-\Delta i_{\text{subi}}}}{i_{fg}} \quad (4.70)$$

$$X_i = \begin{pmatrix} -0.13 \\ -0.17 \\ -0.24 \\ -0.39 \\ -0.41 \end{pmatrix}$$

$$\text{Outlet Condition: } X_o := \frac{\overrightarrow{-\Delta i_{\text{subo}}}}{i_{fg}}$$

$$X_o = \begin{pmatrix} -0.09 \\ -0.13 \\ -0.2 \\ -0.34 \\ -0.37 \end{pmatrix}$$

$$f_p := \overrightarrow{(.7249 + .099 p \cdot e^{-.032 \cdot p})} \quad (8.27)$$

$$b := .6 \quad \text{for } D < 1 \text{ cm}$$

$$f_p = \begin{pmatrix} 0.8 \\ 0.9 \\ 1.1 \\ 1.7 \\ 1.8 \end{pmatrix}$$

$$\phi_{\text{crBi}} := 10^4 \cdot \frac{1.883 \cdot 10^3}{\left(\frac{D}{\text{cm}}\right)^b \cdot \left(G \frac{\text{cm}^2 \cdot \text{s}}{\text{gm}}\right)^{.1667}} \cdot \left[\frac{f_p}{\left(G \frac{\text{cm}^2 \cdot \text{s}}{\text{gm}}\right)^{.1667}} - X_o \right] \quad (8.27)$$

$$\phi_{\text{crBi}} = \begin{pmatrix} 2.9 \times 10^6 \\ 3.5 \times 10^6 \\ 4.6 \times 10^6 \\ 7.2 \times 10^6 \\ 7.5 \times 10^6 \end{pmatrix} \quad \text{Watt/m}^2$$

Calculation of Comparative Critical Heat Flux for Pool Boiling at 1 Atm:

Calculation at 1 atm and 19 atm, saturation conditions:

$$k := \frac{\pi}{24}$$

1 atm	19 atm
$\rho_{f1} := 958 \frac{\text{kg}}{\text{m}^3}$	$\rho_{f2} := 853 \frac{\text{kg}}{\text{m}^3}$
$\sigma_1 := .05878 \frac{\text{N}}{\text{m}}$	$\sigma_2 := .0355 \frac{\text{N}}{\text{m}}$
$\rho_{g1} := .598 \frac{\text{kg}}{\text{m}^3}$	$\rho_{g2} := 9.588 \frac{\text{kg}}{\text{m}^3}$
$c_{p1} := 4.218 \frac{\text{joule}}{\text{gm} \cdot \text{K}}$	$c_{p2} := 4.55 \frac{\text{joule}}{\text{gm} \cdot \text{K}}$
$i_{fg1} := 2257 \frac{\text{joule}}{\text{gm}}$	$i_{fg2} := 1900 \frac{\text{joule}}{\text{gm}}$

$$\phi_{\text{crPo}} := \left[\left(k \cdot i_{fg} \right) \cdot \left(\rho_g \right)^{.5} \cdot \left[\sigma \cdot g \cdot \left(\rho_{fi} - \rho_g \right) \right]^{.25} \right] \quad (4.58)$$

$$\phi_{\text{crPo}} = \left(\frac{1.1 \times 10^6}{3.3 \times 10^6} \right) \text{kg s}^{-3}$$

Calculation at 1 atm (100C sat) and 19 atm (210C sat), exit temperature,
 T_{fL} subcooled conditions:

$$T_{\text{fL}} = 307.3\text{K} \quad \text{Exit Temperature}$$

$$\Delta T_{\text{sub}1} := 48 \cdot \text{K} \quad \Delta T_{\text{sub}2} := 158 \cdot \text{K}$$

$$B := \left[.1 \cdot \left(\frac{\rho_f}{\rho_g} \right)^{.75} \cdot \left(\frac{c_p}{i_{fg}} \right) \right] \quad (4.63)$$

$$B = \left(\frac{0.047}{6.937 \times 10^{-3}} \right) \text{K}^{-1}$$

$$\phi_{\text{crPoSub}} := \phi_{\text{crPo}} \cdot (1 + B \cdot \Delta T_{\text{sub}})$$

$$\phi_{\text{crPoSub}} = \left(\frac{4.88 \times 10^6}{1.45 \times 10^7} \right) \frac{\text{watt}}{\text{m}^2}$$

VI. EC Materials of Construction:

The material selected for use in the electron collector depends on its durability during exposure to thermal cycling. Factors that affect material suitability for thermal loading are strength and properties that minimize the thermal gradients and strain that develops from thermal loading. The stress σ will be proportional the following properties:

$$\sigma \sim \frac{\alpha}{k \cdot c}$$

where σ =stress, α =coef of expansion, k =conductivity,
 c =specific heat

The materials considered for construction correspond to those evaluated in Reference (7), and included the following:

C17510	Beryllium Copper	Brush Wellman
C18150	Zirconium Chromium Copper	Scot Forge
C15715	Glidcop Dispersion Strengthened Copper AL-15	North American Hoganas SCM Metal Products, Inc.

Material properties have been estimated by the above manufacturers for the tube form to be produced for the EC, and are as follows:

Material	C17510 BeCu	C18150 ZrCrCu	C15715 glidcop	C10200 OFHC
-----	-----	-----	-----	-----
Density, kg/m ³	8830	8900	8900	8950
Modulus of Elasticity, 10 ⁶ psi	20	17.4	19.4	17.0
Conductivity, W/m-C	189	315	354	393
Coefficient of Expansion, ppm/C	17.7	17.1	16.6	17.6
Yield Strength, ksi	80	48	40	10.5
Tensile Strength, ksi	100	57	52	32
Fatigue Strength, ksi (10 ⁸ cycles)	38-44	—	—	—

The following table provides a summary of the thermal and stress response of the EC during 50mS, 10 hz pulsing. Stress values occur at the end of the pulse.

Material	C17510	C18150	C15715
-----	-----	-----	-----
BeCu	ZrCrCu	glidcop	
Temperature Range, degC, (At Max Temp Location)	131-151	119-136	114-131
Stresses:			
Von Mises	40.2	34.7	32.3
Hoop, Max Tension	+28.4	+23.9	+22.2
Max Compression	-47.1	-40.6	-38.0
Axial, Max Tension	+20.3	+17.0	+15.5
Max Compression	-29.7	-25.1	-23.2
Stress Ratio, Yield/VM Stress	1.99	1.38	1.24

Other Factors:

1. Manufacturing Methods. The BeCu parts of the EC will be joined by electron beam welding instead of furnace brazing. Both BeCu and ZrCrCu lose strength if exposed to high temperatures, such as those encountered in the furnace brazing process brazing. Glidcop has the advantage of retaining its strength when exposed to high temperatures
2. Cost. The unit costs for the manufacture of the raw, unmachined EC cylinder, based on producing 2 units at the same time, are:

Material	Estimated Cost
-----	-----
Glidcop	\$20,000
ZrCrCu	\$3,000
BeCu - Std	\$3,800
BeCu - Hycon	\$7,800

Conclusion

Beryllium copper provides the highest margin between the actual stresses developed and yield stress (see Stress Ratio), then Zirconium Chromium Copper, followed by gildcop. A comparison using fatigue strength is not possible, since published values could not be found for ZrCrCu and glidcop. The beryllium copper has published values of 38–44 ksi for fatigue strength, although Brush Wellman will not guarantee these values. Furthermore, the use of a special high purity grade of beryllium copper, Hycon 3, will yield even lower stresses and better fatigue endurance. Hycon has a thermal conductivity equal to at least 65% of OFHC, while C15710 is 48% minimum.

Previous research on the fatigue strength of copper alloys⁷ gives test results for high stress, low cycle (10^6) fatigue for the three alloys above. Although not equivalent to high cycle fatigue, these results corroborate this conclusion, showing hycon 3, beryllium copper providing higher fatigue performance over glidcop AL-25. In these tests the performance of zirconium chromium copper is not much better than OFHC copper, but cannot be used for comparison due to the low hardness of the specimens (14.5 ksi yield strength). The form of ZrCrCu considered for the electron collector has a yield strength of 48 ksi.

References:

1. Heating Rates of Magnetron Cathode, Prelec, K., 1975, AGS Note 6
2. Analysis of Heat and Mass Transfer, Eckert & Drake, 1972
3. Fundamentals of Machine Elements, Hamrock, Jacobson, and Schmidt, McGraw-Hill, 1999, TJ230-H245
4. Guide to Beryllium Copper, Brush Wellman, 2002
5. Strength of Hycon 3 HP and Other Copper Alloys from 20 to 200C, IEEE Trans on Magnets, Vol. 30, No 4, Jul, 1994
6. Convective Boiling and Condensation, Third Edition, Collier & Thome
7. Fatigue Behavior of Copper and Selected Copper Alloys for High Heat Flux Applications, Leedy, Stubbins, Singh, and Garner, Journal of Nuclear Material, 1996
8. Power density distribution_20A_15 keV_45.xls, S. Pikin, 3/2005
9. Subcooled Water Flow Boiling Transition and the L/D Effect on CHF for a Horizontal Uniformly Heated Tube, Boyd, A&M University, Fusion Technology, Sept 1990